Acta Geodyn. Geomater., Vol. 21, No. 1 (213), 83–91, 2024
DOI: 10.13168/AGG.2024.0007
journal homepage: https://www.irsm.cas.cz/acta

ORIGINAL PAPER

COMPARATIVE ANALYSIS OF PCA AND ICA ON TREND ESTIMATION OF SEA-LEVEL CHANGE FROM TIDE GAUGE OBSERVATIONS

Jie WANG [1], Xiaoxing HE [1], Shunqiang HU [2] *, Xiwen SUN [3], Wentao WANG [4] and Huijuan LIU [4]

[1] *School of Civil and Surveying and Mapping Engineering, Jiangxi University of Science and Technology, Ganzhou 341000, China*
[2] *Key Laboratory of Poyang Lake Wetland and Watershed Research, Ministry of Education, Jiangxi Normal University, Nanchang 330022, China*
[3] *School of Surveying and Geoinformation Engineering, East China University of Technology, Nanchang 330013, China*
[4] *Hebei Institute of Investigation and Design of Water Conservancy and Hydropower Co., Ltd, Shijiazhuang, 050085, China*

**Corresponding author's e-mail:* husq@jxnu.edu.cn

ARTICLE INFO

Article history:
Received 4 January 2024
Accepted 22 February 2024
Available online 29 February 2024

Keywords:
Tide Gauge
Sea-Level Change
Trend Estimation
Stochastic Noise
PCA
ICA

ABSTRACT

Sea-level rise directly caused by climate change is impacting coasts around the world and low-lying islands, requiring a continuous accurate monitoring. We analyze the sea-level data observed by 20 tide gauges located in the east coast of the United States of America (USA) over the period January 1972 to December 2021 by using an open-source toolbox SLR_APP. After mitigating noise using Principal Component Analysis (PCA) and Independent Component Analysis (ICA) method, we estimate the trend change and its uncertainty of sea-level considering the stochastic noise properties of the observations. The sea-level estimates and associated uncertainty are smaller than the raw observations after the noise reduction. Our results show that: the average values of the absolute trend change are 1.51 % and 0.82 %, and the mean trend uncertainty are reduced by 44.78 % and 21.26 % after PCA and ICA noise reduction, respectively. We conclude that PCA method performs better than ICA especially in reducing the associated trend uncertainty of the sea level change. Improving the sea-level rise estimation and prediction contribute globally to enhance public safety, in particular for the coastal communities.

1. INTRODUCTION

One of the primary consequences of climate change is the rise in global mean sea-level (GMSL). This natural phenomenon results from the melting of glaciers, land-based ice caps, and the expansion of seawater due to the increase of sea surface temperatures. The scientific community has monitored the sea-level rise (SLR) since 1992. The GMSL has already reached nearly 10.1 centimeters and projections suggest an anticipated rise vary from 0.3 to 0.9 meters by the end of this century (Church and White, 2011; Oppenheimer et al., 2019; Wouters and van de Wal, 2018). Cities located along coastlines worldwide are now facing the impending risks associated with the SLR, including the tidal flooding and the storm-surges (Wahl and Dangendorf, 2022). In response to the escalating threat of climate change, governments and local authorities have developed strategic plans aimed at fortifying climate resilience and adaptation for coastal communities and businesses vulnerable to environmental hazards. These proactive measures are crucial in preparing for potential natural disasters, mitigating associated economic and human costs (Walkden, 2022).

Geodetic observations play a pivotal role in estimating relative sea level rise (RSLR) through tide gauges (TG) (Hannah and Bell, 2012; Raj et al., 2022), which present the sea surface height relative to the crustal reference. However, due to local geodynamic factors such as tectonic activity and subsidence, the observations may encompass various movements, exhibiting linear or non-linear behaviors over extended periods（e.g., glacial isostatic adjustment, inter-seismic strain accumulation),（Camargo et al., 2022; Montillet et al., 2018; Santamaría-Gómez et al., 2012; Wang et al., 2021).

The analysis of multi-decadal or century-long TG records presents numerous challenges in accurately estimating SLR and its associated uncertainty. A meticulous approach is essential, requiring careful modeling of diverse processes (e.g., seasonal variations) and considering the temporally correlated noises intrinsic to these measurements. These noises can impact the analysis of various time series, including geodetic time series (Burgette et al., 2013; He et al., 2017; He et al., 2022a; Montillet and Bos, 2019), particularly affecting observations recorded by TG.

The Principal Component Analysis (PCA) and Independent Component Analysis (ICA) method was used for various signal processing. Therefore, we perform the PCA and ICA method to reduce the coloured and white noises (i.e. temporally correlated noises). This paper is organized as follows: Section 2

Cite this article as: Wang J, He X, Hu S, Sun X, Wang W, Liu H: Comparative analysis of PCA and ICA on trend estimation of sea-level change from tide gauge observations. Acta Geodyn. Geomater., 21, No. 1 (213), 83–91, 2024. DOI: 10.13168/AGG.2024.0007

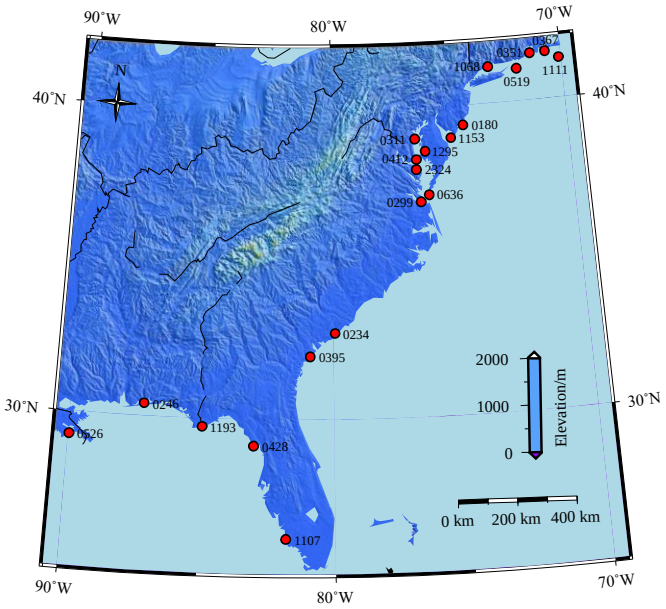

Fig. 1 Spatial distribution of the 20 TG around the east coast of the USA.

mainly describes our TG data and the stochastic noise models, and PCA/ICA method for noise reduction, and open-source toolbox SLR_APP. Section 3 analyzes the trend of sea level changes based on optimal noise model and compares the effects of applying the PCA and ICA algorithms. Section 4 presents the conclusions of our research.

2. DATA AND METHODS

2.1. TIDE GAUGE DATA

The TG data utilized in this study are obtained from the Permanent Service for Mean Sea Level (PSMSL), a global repository for long-term sea-level change information derived from various TG sites (Holgate et al., 2013).

The sea-level estimated from TG is influenced by the vertical land movement (VLM), which can potentially bias SLR values. The VLM is caused by various solid-earth processes, which can be either regional or localized to the tide gauge reference point. These phenomena may originate from either natural or human-induced causes and can manifest as steady-state (linear) or transient (nonlinear) signals over time. Regional processes that exhibit effective linearity over the century-scale duration of the longest instrumental TG records encompass glacial isostatic adjustment and inter-seismic tectonic strain accumulation in the absence of local earthquakes (Wöppelmann and Marcos, 2016).

We specifically select 20 tide gauges located along the east coast of the USA, which smaller than a previous study from Dangendorf et al. (2023), covering a time span from 1972 to 2021. The spatial distribution of these TG is illustrated in Figure 1. To obtain an RSLR, we do not correct the observations from the VLM (Montillet et al., 2018).

2.2. SELECTING OPTIMALLY THE STOCHASTIC NOISE MODEL

2.2.1. STOCHASTIC NOISE MODEL

Within geodetic time series, such as the TG observations, geodynamical processes can pose challenges in terms of accurate modeling and estimation using appropriate functional and stochastic noise models (Dong et al., 2006; Li et al., 2015; Tiampo et al., 2012). Bos et al. (2014) addressed this issue by modeling the stochastic noise properties of TG data, incorporating a trend representing the SLR, and accounting for seasonal variations.

We employ the Auto-Regressive Moving Average (ARMA), the Auto-Regressive Fractionally Integrated Moving Average (ARFIMA), and the Generalized Gauss Markov (GGM) stochastic noise models to analyze the TG data in this paper. These models, as suggested by Bos et al. (2013) and further supported by He et al. (2019) and He et al. (2022b), contribute to a comprehensive understanding of the stochastic noise components within the geodetic time series, enhancing our ability to model and interpret the underlying processes.

2.2.2. OPTIMAL NOISE MODEL SELECTION

The optimal noise model is selected via the information criteria. We employ the BIC_tp criteria (or modified bayesian information criteria) developed by He et al. (2019) to model the noise properties. It was applied to estimate SLR on the west coast of the USA in He et al. (2022b). The optimal noise selection is conducted using the Hector and the additional routines within the software package (Bos et al., 2014; He et al., 2019; He et al., 2021).

2.3. DATA PROCESSING AND STATISTICAL ANALYSIS

We remove outliers from the raw observations with the (3 sigma) Inter Quartile Range (3IQR) method (Bos et al., 2013). 3IQR is a measure of statistical dispersion, which is a useful method to detect outliers in raw TG time series. When using 3IQR, the raw TG time series is split into quartiles. The distances between the upper and lower quartiles are used to determine the IQR (Wan et al., 2014). Bos et al. (2013) and He et al. (2019) have emphasized the positive impact of outlier removal on data quality using various geodetic datasets (TGs and daily position GNSS time series). This process not only diminishes noise scatter, but also holds the potential to yield a more precise and accurate analysis of geodynamical phenomena. Furthermore, we use the so-called "R" coefficient to quantify the impact of noise reduction on the correlation of TG time series. This coefficient can express the correlation before and after the denoising procedure, offering insight into the effectiveness of the outlier removal process in improving the overall coherence of the time series data. The coefficient is defined as:

$$R = \frac{\sum_{i=1}^{n}(x_i-\bar{x})(y_i-\bar{y})}{\sqrt{\sum_{i=1}^{n}(x_i-\bar{x})^2 \sum_{i=1}^{n}(y_i-\bar{y})^2}} \quad (1)$$

Where x_i, y_i represents the TG time series before and after noise reduction, respectively. n is the number of the TG time series. $\bar{x}$, $\bar{y}$ represents the mean values of TG time series x_i, y_i, respectively.

2.4. NOISE REDUCTION METHODS WITH PCA AND ICA

We used PCA and ICA method to mitigating noise on TG data.

Definition of the PCA:

Assume that there are n TG sites, and the number of time observations is m, a matrix X can be defined as:

$$X = \begin{pmatrix} x_1(t_1) & \dots & x_1(t_m) \\ \vdots & \ddots & \vdots \\ x_n(t_1) & \cdots & x_n(t_m) \end{pmatrix} \quad (2)$$

The covariance matrix $C_X = X^T X$. $\bar{v}_i$ (m*1 column vector) is the eigenvector of the covariance matrix, λ_i is the corresponding eigenvalue, the positive singular value $\sigma_i = \sqrt{\lambda_i}$, $i = 1,2,\cdots,r$. X can be calculated by orthogonal function using the following equation:

$$(X^T X)u_i = \lambda_i \bar{v}_i \quad (3)$$

$$X(t_i, x_j) = \sum_{k=1}^{n} a_k(t_i)\, v_k(x_j) \quad (4)$$

$a_k(t_i)$ can be calculated using the following equation:

$$a_k(t_i) = \sum_{j=1}^{n} X(t_i, x_j)\, v_k(x_j) \quad (5)$$

Where $a_k(t)$ is the k-th principal component, $v_k(x)$ represents the spatial response characteristic matrix corresponding to the principal component (He et al., 2015; Dong et al., 2006; Shlens, 2014; Zhu et al., 2024).

Definition of the ICA:

ICA model can be expressed as follows:

$$y = AS + e \quad (6)$$

Where y is the observation time series of each TG site, A is the mixing matrix, S is the independent source, and e is the random error. The ICA model estimates the unmixing matrix $W = A^{-1}$ for maximizing the non-Gaussianity of each source (Hyvarinen, 1999, Hyvärinen, 2013).

2.5. SOFTWARE DEVELOPMENT

The noise analysis within the time series in data preprocessing is essential for accurate estimation of trend. However, there is a limited availability of tools specifically designed for this purpose. To address this shortfall, we redevelop our previous GNSS Time Series Noise Reduction Software (GNSS-TS-NRS (He et al., 2020)) with a new module for sea-level rise application (SLR_APP).

2.5.1. MAIN FEATURES OF THE SLR_APP MODULE

SLR_APP is developed in MATLAB (MATLAB, 2022) and it features a graphical user interface (Hunt et al., 2014). SLR_APP serves as an extension module of the GNSS-TS-NRS software (He et al., 2020). Users can access this tool by utilizing the dedicated "SLR application" button within GNSS-TS-NRS or by running "SLR_Application.m" within the generic MATLAB interface.

2.5.2. DATA DOWNLOAD AND DISPLAY

The SLR_APP main interface is shown in Figure 2a. "TG Data Download" relies on the MATLAB functions to connect the PSMSL website, and we acquire the compressed package containing TG time series data, and subsequently unpack it into a folder. "TS Display" reads TG data in the folder selected by the user, and we can draw the TG time series (see Fig. 2b).

3. RESULTS AND DISCUSSION

3.1. FILTERING THE TG TIME SERIES TO REDUCE THE NOISE

TG time series noise reduction includes the interpolation, detrending, and the ICA/PCA noise reduction. It is inevitable that missing data exist in TG time series. Besides, it is required to ensure the TG time series with consistent length and complete dataset as discussed by Dong et al., (2006) and Burgette et al., (2013). The Regulated EM algorithm (RegEM) was used to interpolate the missing data before the noise reduction, available at "https://github.com/tapios/RegEM.git". This method was proposed by Schneider (2001), which perform ridge regression to achieve regression regularization and

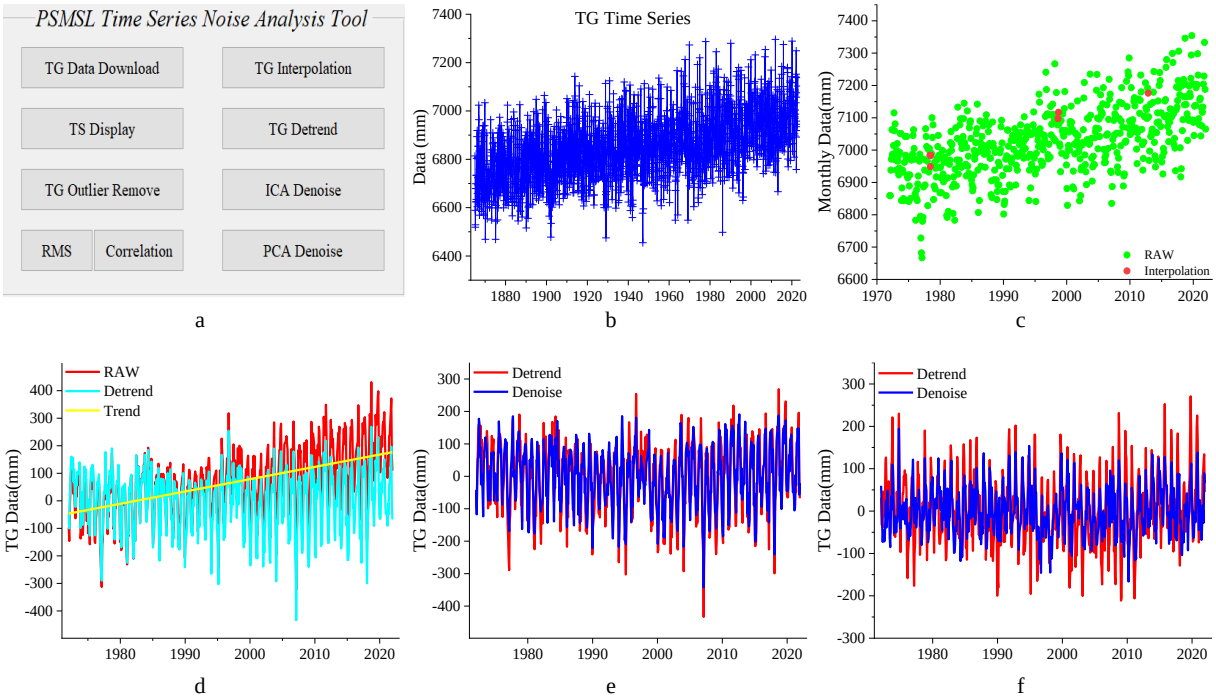

Fig. 2 Overview SLR_APP toolbox (a. main interface, b. drawing TG data, c. time series interpolation, d. detrending TG time series, e. ICA noise reduction, f. PCA noise reduction).

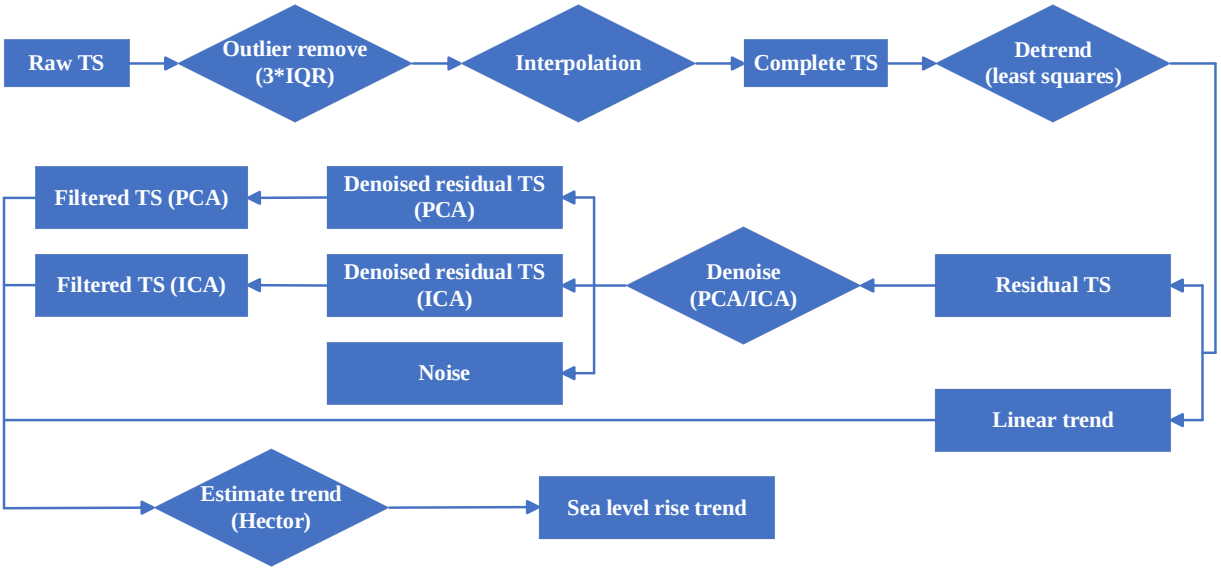

Fig. 3 PCA and ICA applied to the TG observations and SLR trend estimation.

parameter estimation. An example of interpolation is shown in Figure 2c. The goal of noise reduction is to remove noise from residual time series (i.e. time series without the linear trends). To obtain the residuals time series, we perform least squares method to detrend the TG time series, as shown in Figure 2d. Then, we apply the ICA (or PCA) method to mitigate noise. Figure 2e and Figure 2f show some examples of filtered time series with PCA and ICA. The procedure of reducing noise is summarized as follows:

Step 1: Using the 3IQR method remove the outliers from the raw TG time series and time series interpolation.

Step 2: Using the least-squares method detrend the time series for obtaining the residual time series.

Step 3: Performing the PCA/ICA on the residual time series to obtain the residual time series with less noise (also called the denoise time series). Then add the linear trend estimation in step 2 to obtain the filtered time series.

Step 4: Estimating the trend from the filtered time series using the Hector software to obtain SLR trend.

Figure 3 shows the flowchart of the whole process described.

Table 1 Trend and its uncertainty of TGs on optimal models.

Site	Trend (mm/yr)	Site	Trend (mm/yr)
0180	5.41±0.48	0519	5.25±0.40
0234	3.98±0.50	0526	8.06±0.49
0246	3.59±0.44	0636	4.40±0.39
0299	5.55±0.46	1068	3.48±0.44
0311	4.79±0.37	1107	3.56±0.53
0351	3.51±0.32	1111	4.38±0.28
0367	3.94±0.33	1153	5.22±0.36
0395	4.21±0.47	1193	2.83±0.50
0412	5.15±0.51	1295	4.45±0.50
0428	3.91±0.50	2324	5.96±0.43

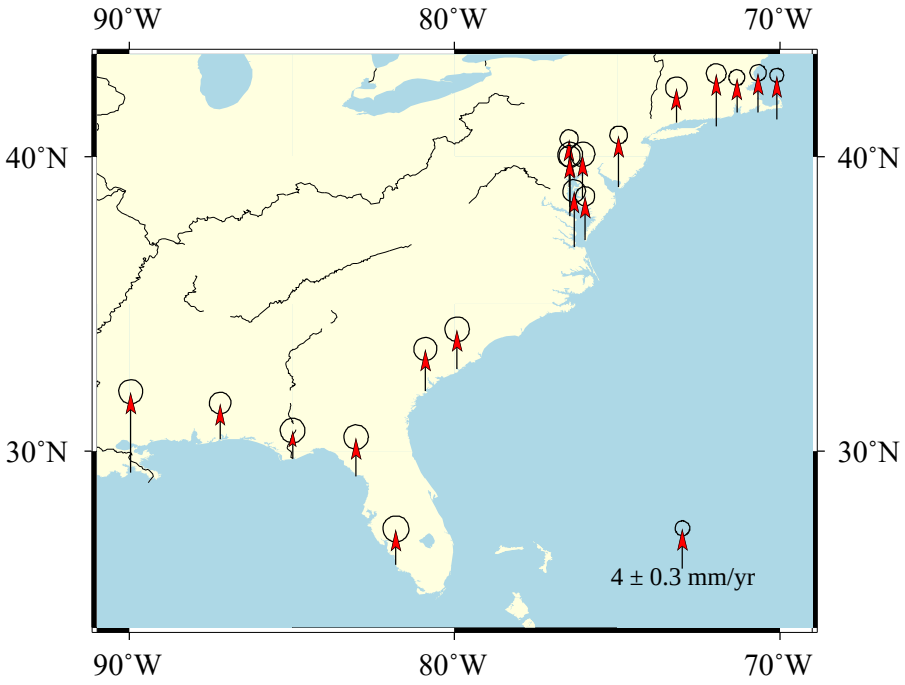

Fig. 4 Estimated SLR (arrow) and associated uncertainty (ellipse) for each TG.

3.2. SEA-LEVEL RATE

We use the BIC_tp criterion to select the optimal model as discussed in the previous section to estimate the RSLR trend and its uncertainty for each TG time series. Table 1 shows the RSLR estimate and associated uncertainty based on the optimal noise models explained in the previous sections. Figure 4 shows the spatial distribution of the RSLR around the east cost of the USA. From the Figure 4 and Table 1, we can see that the mean values of RSLR trend is 4.58±1.16 mm/yr during the last 50 years.

3.3. PERFORMANCE ANALYSIS OF TREND WITH ICA AND PCA

The root mean square (RMS) value of the TG time series is computed with our in-house software discussed in Section 2. Note that the trends and its uncertainty, are computed by the selected optimal model.

Figure 5 shows the RMS value after applying the PCA and ICA algorithm. The RMS of the TG time series has decreased compared with raw TG time series. Table 2 displays the RMS values for each TG. We used two indexes “Diff” and “Percentage” to analyze the result after noise reduction by ICA and PCA method. “Diff” is the difference between the RMS value of the TG raw time series and the RMS value of the denoised time series. “Percentage” represent the“Diff” divided by the RMS value of the raw time series. After the noise reduction with PCA or ICA, the “Diff” mean values are 23.88±10.99 mm and 8.49±5.88 mm, while “Percentage” mean values are approximately 17.36 % and 5.80 %, respectively.

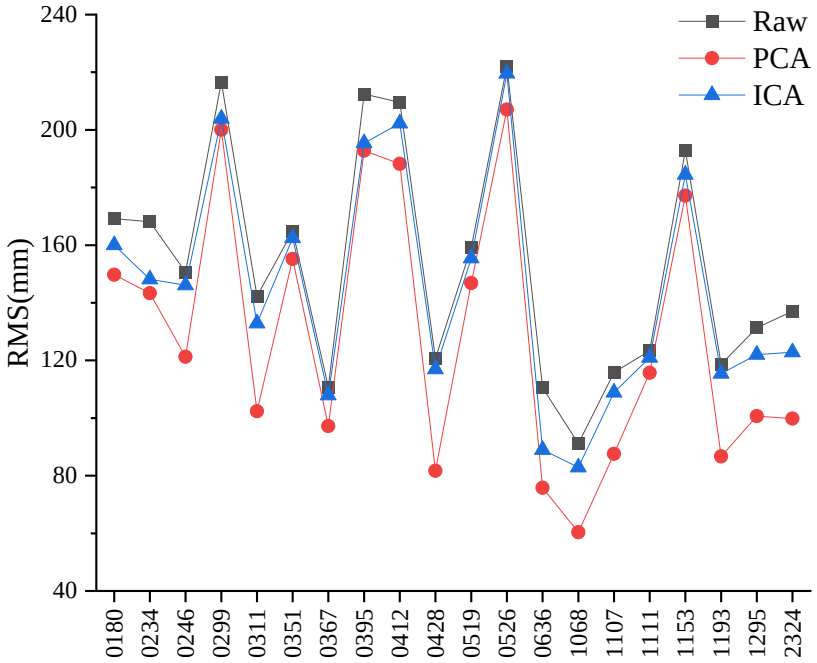

Fig. 5 RMS values for each TG before and after noise reduction.

Table 2 Results of "Diff" and "Percentage".

Values	Diff		Percentage	
	PCA	ICA	PCA	ICA
MAX	39.89	21.47	33.79 %	19.43 %
MIN	7.65	2.38	5.87 %	1.15 %
MEAN	23.88	8.49	17.36 %	5.80 %

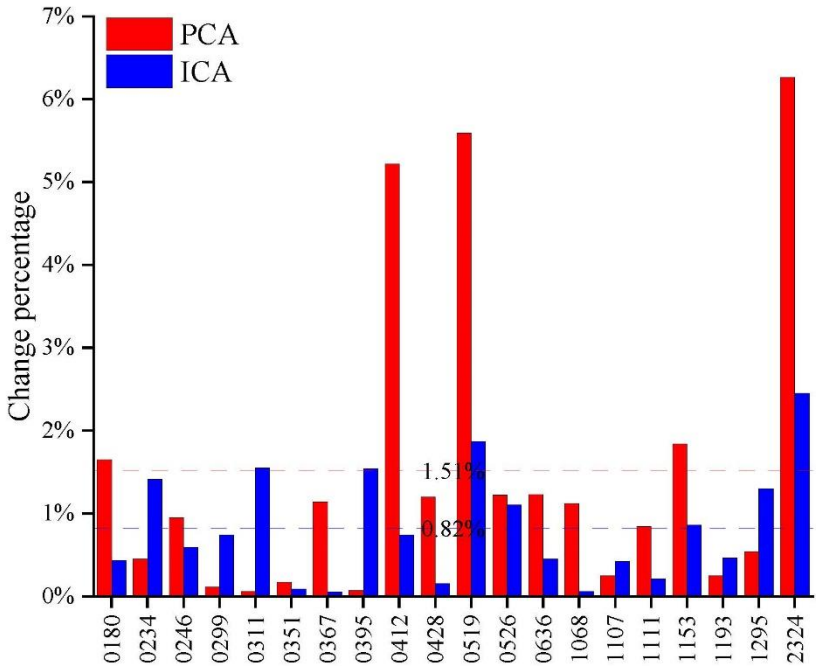

Fig. 6 Trend change percentage (red PCA, blue ICA) for each TG before and after noise reduction.

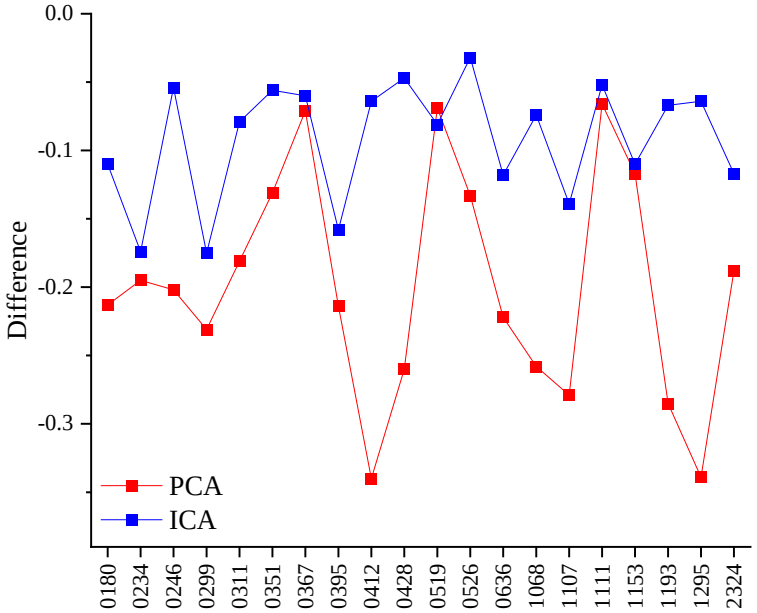

Fig. 7 Trend uncertainty variation before and after noise reduction with PCA (red)/ICA (blue).

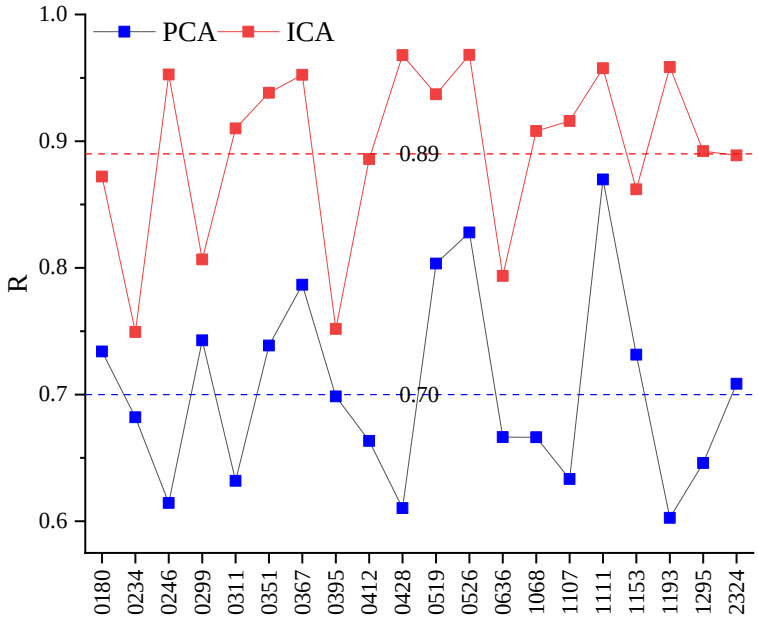

Fig. 8 The R Coefficient between raw and filtered TG time series with PCA (blue) /ICA (red).

To obtain the percentage of trend change, we calculated the absolute difference between the trend of the raw TG time series and the trend after denoising. Then, we divided this difference by the trend of the raw TG time series. The results as shown in Figure 6. After applying the PCA, the largest percentage of trend change is 6.26 %, correspond for the site no 2324, and the mean value is 1.51 %. For ICA, the mean value of trend change percentage is 0.82 %, and the trend change percentage for all sites is less than 3 %.

Figure 7 shows the difference in trend uncertainty before and after noise reduction (after noise reduction minus before noise reduction). Figure 7 shows that the trend uncertainty difference after reducing the noise using either the PCA or the ICA method are less than 0, indicating that the trend uncertainty is reduced. The mean value of difference after PCA and ICA noise reduction is -0.20 mm/yr and -0.09 mm/yr, respectively, and their percentage reductions relative to the raw values is 44.78 % and 21.26 %, respectively.

Figure 8 shows the R coefficient between raw and filtered TG time series with PCA and ICA. The blue curve is the R coefficient between the raw time series and time series after the PCA denoising. The red line corresponds to ICA denoising. The dotted line

represents the average correlation coefficient of the TG. It can be seen from Figure 8 that the correlation value of PCA denoising at all TG sites are greater than ICA denoising. the average correlation value between raw and filtered TG time series with PCA is 0.70, while average correlation value between raw TG time series and denoising time series by ICA is 0.89. Combined with the previous results, the result of PCA denoising have a larger numerical change and better noise reduction effect compared to ICA denoising. ICA may only reduce a smaller percentage of the noise, resulting in a higher correlation with the raw time series.

4. CONCLUSIONS

This study focuses on providing an improved estimation of the RSLR with TG observations, we investigated 20 TGs along the east coast of the USA over past 50 years from 1972 to 2021. Three stochastic models (ARFIMA, ARMA, and GGM) are employed to estimate the trend in the TG observations. A comparative analysis was performed by PCA and ICA denoising. Our main results are:

1. We designed an open-source SLR_APP toolbox to analyze TG data, which takes advantage of the interactive GUI interface in MATLAB. The PCA and ICA denoising algorithms are implemented. The toolbox also includes functions for data downloading, drawing time series, and accuracy evaluation, which together form a complete TG time series denoising analysis tool with good interactivity.
2. The average values of the absolute trend change are 1.51 % and 0.82 %, the mean trend uncertainty is reduced by 44.78 % and 21.26 %, and the mean values of "R" correlation coefficient value are 0.70 and 0.89 after PCA and ICA denoising, respectively. ICA may retain more noise, resulting in a higher correlation with the raw TG time series. The PCA noise reduction have a better result than the ICA noise reduction in our study.
3. The results based on our selected TG time series show that the sea-level on the USA coast is rising over the past 50 years. The mean annual increase in sea level is around 4.58 ± 1.16 mm. Furthermore, regional sea level may greatly vary from one location to the other due to various processes (e.g., local geodynamic, GIA, ocean dynamic). In our study, the RSLR is not corrected from the VLM. Characterizing the spatial variability surrounding the location of each TG is crucial to understanding how coastal sea level varies on interannual to multidecadal time scales. Yet, this remains a key scientific challenge due to the lack of systematic coastal observations (Cazenave et al., 2022). This study is another step to improve the estimation of RSLR applying the PCA and ICA algorithms to reduce the noise on the TG measurements and the estimated SLR. However, some work is required to adapt our methodology to the global network of TGs and also to satellite altimetry observations. We should analyze the difference in the future when correcting the RSLR with VLM, and compared with the satellite altimetry datasets.

ACKNOWLEDGMENTS

The TG data are available at "https://psmsl.org/". This work was sponsored by National Natural Science Foundation of China (42364002), Major Discipline Academic and Technical Leaders Training Program of Jiangxi Province (20225BCJ23014). The SLR_APP toolbox is available at "https://www.kaggle.com/datasets/jiewanglz/slr-app-toolbox-for-tide-gauge".

REFERENCES

Bos, M.S., Fernandes, R.M.S., Williams, S.D.P. and Bastos, L.: 2013, Fast error analysis of continuous GNSS observations with missing data. J. Geod., 87, 4, 351–360. DOI: 10.1007/s00190-012-0605-0

Bos, M.S., Williams, S.D.P., Araújo, I.B. and Bastos, L.: 2014, The effect of temporal correlated noise on the sea level rate and acceleration uncertainty. Geophys. J. Int., 196, 3, 1423–1430. DOI: 10.1093/gji/ggt481

Burgette, R.J., Watson, C.S., Church, J.A., White, N.J., Tregoning, P. and Coleman, R.: 2013, Characterizing and minimizing the effects of noise in tide gauge time series: relative and geocentric sea level rise around Australia. Geophys. J. Int., 194, 2, 719–736. DOI: 10.1093/gji/ggt131

Camargo, C.M., Riva, R.E., Hermans, T.H. and Slangen, A.: 2022, Trends and uncertainties of mass-driven sea-level change in the satellite altimetry era. Earth. Syst. Dynam., 13, 3, 1351–1375. DOI: 10.5194/esd-13-1351-2022

Cazenave, A., Gouzenes, Y., Birol, F., Leger, F., Passaro, M., Calafat, F.M., Shaw, A., Nino, F., Legeais, J.F., Oelsmann, J., Restano, M. and Benveniste, J.: 2022, Sea level along the world's coastlines can be measured by a network of virtual altimetry stations. Commun. Earth. Environ., 3, 1, 117. DOI: 10.1038/s43247-022-00448-z

Church, J.A. and White, N.J.: 2011, Sea-level rise from the late 19th to the early 21st century. Surv. Geophys., 32, 585–602. DOI: 10.1007/s10712-011-9119-1

Dangendorf, S., Hendricks, N., Sun, Q., Klinck, J., Ezer, T., Frederikse, T., Calafat, F.M., Wahl, T. and Törnqvist, T.E.: 2023, Acceleration of US Southeast and Gulf coast sea-level rise amplified by internal climate variability. Nat. Commun., 14, 1, 1935. DOI: 10.1038/s41467-023-37649-9

Dong, D., Fang, P., Bock, Y., Webb, F., Prawirodirdjo, L., Kedar, S. and Jamason, P.: 2006, Spatiotemporal filtering using principal component analysis and Karhunen-Loeve expansion approaches for regional GPS network analysis. J. Geophys. Res., Solid Earth, 111, B3. DOI: 10.1029/2005JB003806

Hannah, J. and Bell, R.G.: 2012, Regional sea level trends in New Zealand. J. Geophys. Res., Oceans, 117, C1. DOI: 10.1029/2011JC007591

He, X., Bos, M.S., Montillet, J.P. and Fernandes, R.M.S.: 2019, Investigation of the noise properties at low frequencies in long GNSS time series. J. Geod., 93, 9, 1271–1282.DOI: 10.1007/s00190-019-01244-y

He, X., Bos, M.S., Montillet, J.P., Fernandes, R., Melbourne, T., Jiang, W. and Li, W.: 2021, Spatial variations of stochastic noise properties in GPS time series. Remote Sens., 13, 22, 4534. DOI: 10.3390/rs13224534

He, X., Hua, X., Yu, K., Xuan, W., Lu, T., Zhang, W. and Chen, X.: 2015, Accuracy enhancement of GPS time seriel using principal component analysis and block spatial filtering. Adv. Space Res., 55, 5, 1316–1327. DOI: 10.1016/j.asr.2014.12.016

He, X., Montillet, J.P., Fernandes, R., Bos, M., Yu, K., Hua, X. and Jiang, W.: 2017, Review of current GPS methodologies for producing accurate time series and their error sources. J. Geodyn., 106, 12-29. DOI: 10.1016/j.jog.2017.01.004

He, X., Montillet, J.P., Li, Z., Kermarrec, G., Fernandes, R. ans Zhou, F.: 2022a, Recent advances in modelling geodetic time series and applications for Earth Science and Environmental Monitoring. Remote Sens., 14, 23, 6164. DOI: 10.3390/rs14236164

He, X., Montillet, J.P., Fernandes, R., Melbourne, T.I., Jiang, W. and Huang, Z.: 2022b, Sea level rise estimation on the Pacific coast from Southern California to Vancouver Island. Remote Sens., 14, 17, 4339. DOI: 10.3390/rs14174339

He, X., Yu, K., Montillet, J.P., Xiong, C., Lu, T., Zhou, S., Ma, X., Cui, and H. Ming, F.: 2020, GNSS-TS-NRS: An Open-source MATLAB-Based GNSS time series noise reduction software. Remote Sens., 12, 21, 3532. DOI: 10.3390/rs12213532

Holgate, S.J., Matthews, A., Woodworth, P.L., Rickards, L.J., Tamisiea, M., Bradshaw, E., Foden, P.R., Gordon, K.M., Jevrejeva, S. and Pugh, J.: 2013, New data systems and products at the permanent service for mean sea level. J. Coast. Res., 29, 3, 493–504. DOI: 10.2307/23486334

Hunt, B.R., Lipsman, R.L. and Rosenberg, J.M.: 2014, A guide to MATLAB: for beginners and experienced users. Cambridge University Press.

Hyvarinen, A.: 1999, Fast and robust fixed-point algorithms for independent component analysis. IEEE Trans. Neural Net., 10, 3, 626–634. DOI: 10.1109/72.761722

Hyvärinen, A.: 2013, Independent component analysis: recent advances. Philos. T. R. Soc A., 371, 1984. DOI: 10.1098/rsta.2011.0534

Li, W., Shen, Y. and Li, B.: 2015, Weighted spatiotemporal filtering using principal component analysis for analyzing regional GNSS position time series. Acta Geod. Geophys., 50, 419-436. DOI: 10.1007/s40328-015-0100-1

MATLAB (2020) version 9.8.0.1417392: R2020a, The MathWorks Inc., Natic

Montillet, J.P. and Bos, M.S. (Eds.): 2019, Geodetic time series analysis in Earth sciences. Springer Geophysics.

Montillet, J.P., Melbourne, T.I. and Szeliga, W.M.: 2018, GPS vertical land motion corrections to sea‐level rise estimates in the Pacific Northwest. J. Geophys. Res., Oceans, 123, 2, 1196–1212. DOI: 10.1002/2017JC013257

Oppenheimer, M., Glavovic, B., Hinkel, J., van de Wal, R., Magnan, A.K., Abd-Elgawad, A., Cai, R., Cifuentes-Jara, M., Deconto, R.M., Ghosh, T., Hay, J., Isla, F., Marzeion, B., Meyssignac, B. and Sebesvari, Z.: 2019, Sea level rise and implications for low Lying islands, coasts and communities. IPCC Special Report on the Ocean and Cryosphere in a Changing Climate, Cambridge University Press, 321–445. DOI: 10.1017/9781009157964.006

Raj, N., Gharineiat, Z., Ahmed, A.A.M. and Stepanyants, Y.: 2022, Assessment and prediction of sea level trend in the South Pacific Region. Remote Sens., 14, 4, 986. DOI: 10.3390/rs14040986

Santamaría-Gómez, A., Gravelle, M., Collilieux, X., Guichard, M., Míguez, B.M., Tiphaneau, P. and Wöppelmann, G.: 2012, Mitigating the effects of vertical land motion in tide gauge records using a state-of-the-art GPS velocity field. Global. Planet. Change., 98, 6–17. DOI: 10.1016/j.gloplacha.2012.07.007

Schneider, T.: 2001, Analysis of incomplete climate data: Estimation of mean values and covariance matrices and imputation of missing values. J. Climate., 14, 5, 853–871. DOI: 10.1175/1520-0442(2001)014

Shlens, J.: 2014, A tutorial on principal component analysis. arXiv:1404.1100. DOI: 10.48550/arXiv.1404.1100

Tiampo, K.F., Mazzotti, S. and James, T.S.: 2012, Analysis of GPS measurements in eastern Canada using principal component analysis. Pure Appl. Geophys., 169, 1483–1506. DOI: 10.1007/s00024-011-0420-1

Wahl, T. and Dangendorf, S.: 2022, Regional Sea Level. In Oxford Research Encyclopedia of Climate Science.

Walkden, P.: 2022, Complexities of coastal resilience. Nat. Geosci., 5, 1, 1–1. DOI: 10.1038/s41561-021-00884-0

Wan, X., Wang, W., Liu, J. and Tong, T.: 2014, Estimating the sample mean and standard deviation from the sample size, median, range and/or interquartile range. BMC. Med. Res. Methodol., 14, 135. DOI: 10.1186/1471-2288-14-135

Wang, J., Church, J.A., Zhang, X. and Chen, X.: 2021, Reconciling global mean and regional sea level change in projections and observations. Nat. Commun., 12, 1, 990. DOI: 10.1038/s41467-021-21265-6

Wouters, B. and van de Wal, R.S.W.: 2018, Global sea-level budget 1993--present. Earth. Syst. Sci. Data., 10, 3, 1551–1590. DOI: 10.5194/essd-10-1551-2018

Wöppelmann, G. and Marcos, M.: 2016, Vertical land motion as a key to understanding sea level change and variability. Rev. Geophys., 54, 1, 64–92. DOI: 10.1002/2015RG000502

Zhu, H., Chen, K., Chai, H., Ye, Y. and Liu, W.: 2024. Characterizing extreme drought and wetness in Guangdong, China using global navigation satellite system and precipitation data. Satellite Navigation, 5, 1. DOI: 10.1002/wics.101